Proc. Natl. Acad. Sci. USA
Vol. 89, pp. 75–79, January 1992
Biophysics

Chromophore–protein interactions and the function of the photosynthetic reaction center: A molecular dynamics study

H. TREUTLEIN†, K. SCHULTEN†, A. T. BRÜNGER‡, M. KARPLUS§, J. DEISENHOFER¶, AND H. MICHEL‖

†Department of Physics and Beckman Institute, University of Illinois at Urbana–Champaign, Urbana, IL 61801; ‡Howard Hughes Medical Institute and Department of Molecular Biophysics and Biochemistry, Yale University, New Haven, CT 06511; §Department of Chemistry, Harvard University, Cambridge, MA 02138; ¶Howard Hughes Medical Institute and Department of Biochemistry, University of Texas Southwestern Medical Center, Dallas, TX 75235-9050; and ‖Max-Planck-Institut für Biophysik, D-6000 Frankfurt/Main 71, Federal Republic of Germany

Contributed by M. Karplus, December 26, 1990

ABSTRACT **The coupling between electron transfer and protein structure and dynamics in the photosynthetic reaction center of *Rhodopseudomonas viridis* is investigated. For this purpose molecular dynamics simulations of the essential portions (a segment of 5797 atoms) of this protein complex have been carried out. Electron transfer in the primary event is modeled by altering the charge distributions of the chromophores according to quantum chemical calculations. The simulations show (*i*) that fluctuations of the protein matrix, which are coupled electrostatically to electron transfer, play an important role in controlling the electron transfer rates and (*ii*) that the protein matrix stabilizes the separated electron pair state through rapid (200 fs) and temperature-independent dielectric relaxation. The photosynthetic reaction center resembles a polar liquid in that the internal motions of the whole protein complex, rather than only those of specific side groups, contribute to *i* and *ii*. The solvent reorganization energy is about 4.5 kcal/mol. The simulations indicate that rather small structural rearrangements and changes in motional amplitudes accompany the primary electron transfer.**

Photosynthetic reaction centers (RCs) are protein–chromophore complexes in plant and bacterial membranes. Their function is the conversion of light into a separation of negative and positive charges on different sides of the membrane. The RCs carry out their function with a quantum yield near unity—i.e., each photon absorbed yields a pair of separated charges. Such a high quantum yield does not necessarily lead to high efficiency since this is determined by the quantum yield and the energy content of the separated charge pair relative to the energy of the photon. In fact, high energy efficiency can be realized for small quantum yields when the energy content of the separated charges is increased. A comparison with solar cells shows that the RCs in plants and photosynthetic bacteria are optimized towards high quantum yields as well as towards high efficiencies—e.g., the RC of the photosynthetic bacterium *Rhodopseudomonas viridis* has a quantum yield $q > 0.98$ (1) and an energy efficiency $\phi = 0.1$, whereas optimal solar cells have quantum yields of about $q = 0.5$ and energy efficiencies of about $\phi = 0.3$ (2). An important reason for the emphasis on a high quantum yield in the biological systems may be the need to avoid harmful side reactions, such as the formation of triplet intermediates and, possibly, singlet oxygen.

To achieve a quantum yield near unity, the reactions involved must form a series of intermediates, and the forward reactions initiated by light excitation must be much faster than any back reactions. In the present investigation we initiate an investigation of the relation of the thermal motion of the components of photosynthetic RCs to electron transfer rates. We demonstrate that a strong coupling between such motions and electron transfer exists and that in this respect the RCs resemble weakly polar solvents with rapid dielectric relaxation. The concept that the coupling between thermal motions of charges and dipoles in liquids and proteins plays a role in electron transfer is not new. The basic ideas go back to the work of Marcus (3–5) with more recent contributions by many others, as reviewed in ref. 6. In the present study we extend the earlier work by using molecular dynamics (MD) simulations to provide a microscopic description for the largely phenomenological concepts of the existing models. Such investigations have become feasible through the availability of high-resolution structures for RCs of the purple bacteria *Rp. viridis* (7–9) and *Rhodobacter sphaeroides* (10–12).

The RC complex of *Rp. viridis* consists of four different protein subunits, called cytochrome, L, M, and H. In addition, it contains 14 major cofactors: four heme groups are covalently attached to the cytochrome subunit; four bacteriochlorophyll b, two bacteriopheophytin b, one menaquinone 9, one ubiquinone 9, one nonheme iron, and one carotenoid molecule are associated with the subunits L and M (see Fig. 1). Absorption of light energy by a complex of two bacteriochlorophyll b molecules, the special pair (BCLP and BCMP), leads to a sequence of electron transfer steps within the RC and to a charge separation across the bacterial inner membrane (for reviews, see refs. 13 and 14). The first of these transfers, from the special pair to one of the bacteriopheophytins (BPL), is very rapid (≈3 ps; ref. 15) compared to the back transfer (≈10 ns; ref. 13). This step has been observed to require no activation energy, and its rate increases by as much as a factor of 2 when the temperature is lowered (16). The next electron transfer step, from the bacteriopheophytin to one of the quinones (QA), is also much faster (≈200 ps; refs. 13 and 14) than the back transfer. Recent experiments have been interpreted as providing evidence that the electron transfer to the bacteriopheophytin may involve a short-lived intermediate ionization of the bacteriochlorophyll BCLA (17); however, the results do not appear to be conclusive. The following considerations apply irrespective of the existence of such an intermediate.

The observed electron transfer rates can be described phenomenologically in terms of existing electron transfer theories (e.g., see refs. 5 and 6). In the present report we demonstrate by means of MD simulations that there is a strong coupling between the fluctuating electrostatic interactions of the charges localized on the chromophores and the protein matrix. The importance of protein fluctuations (i.e., low-frequency modes) in electron transfer has been suggested previously (18–21), though specific results concerning their role in determining electron transfer rates are not available. We report here the results of MD simulations of a large (5797 atoms) portion of the RC, including both the

The publication costs of this article were defrayed in part by page charge payment. This article must therefore be hereby marked "*advertisement*" in accordance with 18 U.S.C. §1734 solely to indicate this fact.

Abbreviations: MD, molecular dynamics; RC, reaction center.

functional and the nonfunctional branch (12). A series of simulations were done for the system prior to and after electron transfer to determine the equilibrium structures and fluctuations as well as the relaxation induced by the reaction. Both room temperature and 10 K simulations were performed.

Preliminary reports on simulations at 300 K have been given by us in refs. 22–24. The present work is a significant extension of these studies.** Related work has been performed by Warshel and coworkers (29–31).††

Methods

The calculations we describe in this article were based on the x-ray structure of the RC of *Rp. viridis* at 2.3-Å resolution (J.D., O. Epp, I. Sinning, and H.M., unpublished work). We used charge distributions of neutral and ionized chromophores determined by INDO calculations (32), which are in good agreement with ESR observations that exhibit an asymmetrical distribution of the positive charge between the two monomeric chlorophylls of the special pair. For the excited state of the special pair SP*, we used the ground state charge distribution; the differences between the ground and the excited state of the neutral pair is expected to have a small effect. The MD calculations were made with the CHARMM program (33) and employed the stochastic boundary method to limit the simulation region (34) to the central part of the RC. A spherical shell of atoms 2.5 Å thick around that MD region was treated by Langevin dynamics to approximate the thermal and frictional effects of the surrounding bath. A total of 5726 atoms inside a sphere of 29 Å around the center of mass of the porphyrin rings of the special pair and the bacteriopheophytins were included; all chromophores except the three more distant heme units of the cytochrome are inside the boundary. The simulated protein segment also contains 74 water molecules, which were present in the x-ray structure. In addition, the electrostatic interactions between the protein and charged residues outside the simulated sphere, but within a distance of 37.5 Å from the center, have been taken into account during the simulations. These charged residues, which were kept fixed, neutralize the net charge of the simulated region so as to prevent unphysical effects of electrostatic repulsion.

Fig. 1 displays the average chromophore structure after electron transfer inside the simulated protein segment (reaction and buffer region) together with their abbreviated names. Light is absorbed by the special pair (BCLP and BCMP). Then an electron is transferred from the special pair to the bacteriopheophytin BPL, from there via the menaquinone QA to a ubiquinone QB. Fig. 1 also shows chromophores not directly involved in electron transfer, a carotenoid NS1, a fourth bacteriochlorophyll BCMA, and a second bacteriopheophytin BPM. The chromophores BCMP, BCMA, and BPM are referred to as the "nonfunctional branch" of the RC chromophores; BCLP, BCLA, BPL, and QA are referred to as the "functional branch."

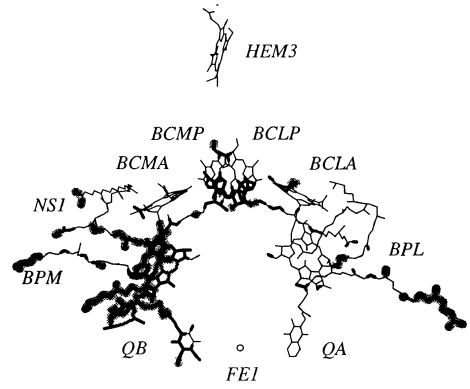

FIG. 1. Average structure of chromophores, together with their abbreviated names in the simulated protein segment after electron transfer. Thin black lines denote atom pairs with at least one atom whose positions have changed by <0.4 Å, shaded areas correspond in the same way to atoms whose positions have changed between 0.4 Å and 0.7 Å, and thick black lines mark atoms with positional changes of >0.7 Å.

To investigate the characteristics of the RC dynamics and to simulate the RC's response to electron transfer, a series of simulations was performed. After equilibrating the system for 20 ps at 300 K, a 20-ps simulation was made to examine the motions of the RC before the primary electron transfer; in this simulation the special pair and the bacteriopheophytin were in the neutral state (22). An electron was then transferred instantaneously (sudden approximation) from the highest occupied orbital of the special pair dimer to the lowest unoccupied orbital of the functional bacteriopheophytin. The positive charge of the special pair was asymmetrically distributed in the porphyrin rings of BCLP (net charge = 0.62) and BCMP (net charge = 0.38) (32). With this chromophore charge distribution, a 20-ps simulation was carried out, and the changes resulting from the charge perturbation were analyzed by comparing the results with those obtained from the simulation with the neutral chromophores. All calculations have been repeated at least twice to reduce statistical errors due to the initial conditions.

Calculations at 10 K were prepared by minimizing a structure with the neutral special pair from the simulation described above. The resulting coordinate set was then equilibrated at 10 K for 20 ps. Subsequently, simulations were performed both for charge distributions corresponding to the neutral and the ionized chromophores for a period of 1 ps each [i.e., a period significantly longer than the time constants of about 100 fs, which govern the dielectric fluctuation and relaxation (see below)].

The rate of electron transfer can be approximated in terms of a first-order perturbation formulation that makes use of a classical trajectory approach, which was first applied to the triplet–singlet isomerization in ethylene (35) and has recently been used to model the forward reaction in the RC (29, 30). In the Marcus formulation of electron transfer (5), this corresponds to the classical limit in which a transition between neutral and ionic states occurs only at crossings of

**The earlier reports were based on a less refined x-ray structure at 3-Å resolution (7, 8) that does not include water bound inside the protein or the ubiquinone and carotenoid prosthetic groups. In contrast to the simulations presented here, the earlier calculations assumed a deprotonated state of the glutamic acid L104, which most likely is protonated and forms a hydrogen bond to the bacteriopheophytin (25), the first or second (17) electron acceptor. In our earlier calculations (22, 26), we used MOPAC (27, 28) charge distributions, which assumed a symmetrical charge on the special pair. The results of MD simulations based on the 2.3-Å resolution structure (J.D., O. Epp, I. Sinning, and H.M., unpublished results) using such charge distribution were similar to those represented in this article. The present calculations also include a larger protein segment (5797 atoms instead of 3634 in the former simulation), which enables us to represent the chromophores of the so-called functional and nonfunctional branch (see, for example, ref. 9; the structure of the photosynthetic RC is available in the Protein Data Bank, Brookhaven National Laboratory) to the same extent.

††MD simulations of the primary electron transfer processes in the RC of *Rb. sphaeroides* at 100 K have been reported by Warshel and coworkers (29–31). The simulations included a study of the electron transfer from bacteriopheophytin to menaquinone in *Rp. viridis*. The simulation in ref. 31 lead the authors to predict the temperature dependence of the transfer rate without actually simulating the protein at different temperatures. Our simulations, contrary to the assumptions underlying the analysis in ref. 31, reveal shifts of average protein properties with temperature.

energy surfaces (35). One can also obtain transfer rates by employing the results of MD simulations [i.e., the energy difference $\Delta E(t)$ introduced below] as input to a quantum mechanical two-level description of the electron transfer (36).

Rigidity and Flexibility

We discuss first some of the significant aspects of the dynamics observed in the simulation at room temperature and then consider their relation to the rate of the back reaction. The thermal motions of protein atoms can be characterized most simply by the rms fluctuations relative to the average structure. The overall rms values are 0.52 Å for the whole RC and 0.33 Å for the C^α atoms. The special pair ring structure is the most rigid of the chromophores (rms < 0.4 Å). This rigidity might be important for the function of the special pair. The phytol chains are found to be most flexible (rms ≈ 0.8 Å). It might be significant that the BCLP phytol chain is in contact with the bacteriopheophytin electron acceptor. The nonfunctional chromophores are slightly more flexible (rms = 0.55 Å) than the chromophores of the functional branch (rms = 0.45 Å). The calculated rms values are in good agreement with the B factors observed in x-ray analysis (J.D., O. Epp, I. Sinning, and H.M., unpublished work). There is no statistically significant difference in mobility before and after electron transfer.

In Fig. 1, we present the average structure after electron transfer. The root mean structural difference with respect to the average structure before transfer is 0.53 Å for all atoms and 0.25 Å for C^α atoms. The magnitude of structural changes due to electron transfer is represented by different ways of indicating the bonds between atoms in Fig. 1 (see *Legend*). The largest structural differences arise for the pheophytin BPM, the ubiquinone QB, and the phytol chains of the nonfunctional chromophores. The structure of all functional chromophores remains essentially unchanged; the average displacements of their ring systems are smaller than their thermal fluctuations. Since the relative reorientations of the chromophores BCMP, BCLA, and BPL are small, they are not likely to control the electron transfer. However, the low flexibility of the functional chromophores and their orientational stability to perturbations (like the electron transfer) is in accord with the suggestion that the geometrical alignment of these functional chromophores is highly optimized for the forward electron transfer (37).

In addition to the average mobility of each chromophore, their relative motions are also important. For all chromophores we have calculated the covariances C_{ik}, the normalized equal time correlation functions between fluctuations of pairs of atoms i and k. C_{ik} makes it possible to differentiate between portions of the protein for which thermal fluctuations do not alter the interchromophore distances significantly ($C_{ik} \approx 1$) and those that do ($C_{ik} < 0$). In general, there are rather strong correlations ($C_{ik} \approx 0.5$) among different chromophores that are within 10 Å of each other. Fig. 2 provides an example of the covariances between the bacteriopheophytin BPL and BCLP, the active branch bacteriochlorophyll in the special pair. Although there is little correlation between the rings of BCLP and BPL, the motion of the phytol chain of BCLP is strongly coupled in phase to the pheophytin ring. The chromophores BCLP, BCLA, and BPL, which are consecutive along the electron transfer pathway, are coupled pairwise in phase. Also, the two special pair chlorophyll ring systems are strongly coupled, which corresponds to the existence of a relatively rigid sandwich complex. Thus, the thermal fluctuations have a small effect on the distances between these chromophores, even though the individual chromophores undergo significant motion. This feature could be important in stabilizing edge-to-edge

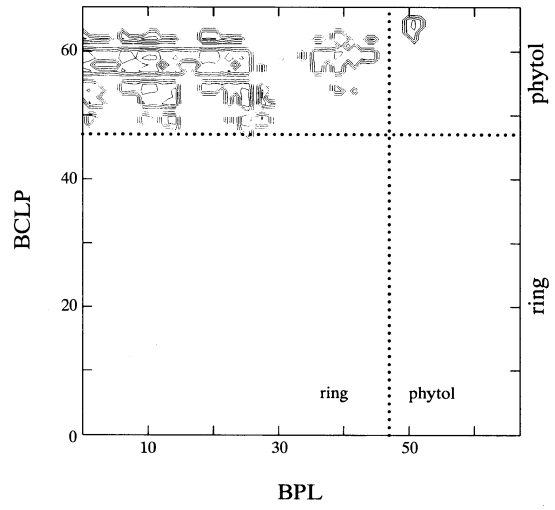

FIG. 2. Covariances C_{ik} between the atoms of BCLP and BPL. The axes present the atomic labels i and k. All correlations C_{ik} are positive. The blank area denotes pairs of atoms i,k with correlations <0.3. Contour lines, which separate regions with larger correlations are shown; the contour lines correspond to increments of 0.1.

contacts between the chromophores, which may be involved in optimal coupling for electron transfer (38).

Dielectric Fluctuations and Dielectric Relaxation

Due to Coulomb interactions between the chromophores and the surrounding protein matrix, the energy difference between the neutral (reactant) and ionic (product) states fluctuates as a function of the thermal motion of the protein. This energy difference controls the quantum mechanical process of electron transfer; therefore, a significant coupling between protein motions and electron transfer can be expected (18). We consider the contribution of the chromophore–protein electrostatic interactions to the difference in energy between the ionic (SP^+ and BPL^-) and neutral (SP* and BPL) states before and after electron transfer. Of interest for the primary electron transfer is the energy difference $\Delta E = E(SP^+ - BPL^-) - E(SP^* - BPL)$. We have set the average value of ΔE prior to electron transfer equal to zero to provide a reference point. The energies not in ΔE (namely, the excitation energy of the special pair, the intramolecular redox energies of the special pair and of the bacteriopheophytin, and the Born energy contribution) must nearly balance the interaction energy with the protein to make the electron transfer possible without large fluctuations in thermal energies. However, as discussed below, the dielectric fluctuations of the protein components provide an energy contribution during the transition, which makes an exact balance of energies unnecessary.

Fig. 3 shows fluctuatious in ΔE as a function of time both before and after electron transfer in the room temperature simulation. The rms fluctuations of $\Delta E(t)$ are of the order of 5 kcal/mol. This value is much larger than the electronic tunneling matrix elements for which values around $10^{-4} - 10^{-3}$ eV (1 eV = 1.602×10^{-19} J) have been assumed. Thus, the fluctuations can bring reactant and product states sufficiently out of resonance to act as an essential control factor for electron transfer.

In the simple perturbation model (5, 29, 30, 35), electron transfer occurs at any time a zero crossing occurs in Fig. 3 (i.e., at the instances when no thermal energy is required for the transfer). Fourier analysis of $\Delta E(t)$ yields a broad frequency distribution without dominant frequency bands. In the low frequency (20 ps^{-1}) the results correspond to the Fourier spectrum of a stochastic Ornstein–Uhlenbeck pro-

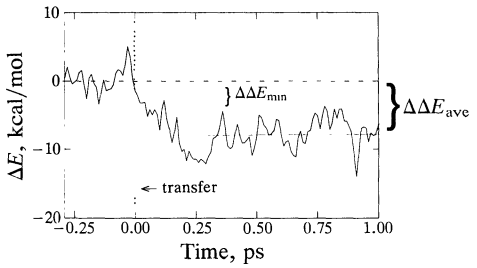

FIG. 3. Energy difference ΔE before and after electron transfer from the special pair to BPL at a temperature of 300 K. The instant the electron is transferred by changing the charge distribution on the special pair and BPL is denoted by an arrow. $\Delta\Delta E_{min}$, minimum $\Delta\Delta E$ value; $\Delta\Delta E_{ave}$, average $\Delta\Delta E$ value.

cess (i.e., Brownian motion in a harmonic potential), but there are also significant high-frequency components as described in ref. 36. At the point marked by an arrow (at 0 ps), the electron was transferred instantaneously and a simulation with the new charge distribution was initiated. Within 200 fs after the transfer, $\Delta E(t)$ decreases by about 10 kcal/mol and then fluctuates around a new mean value, 8.5 kcal/mol below the average before transfer. The energy decrement $\Delta\Delta E$ can be interpreted as solvation of the separated charge pair by the protein matrix. The very rapid initial relaxation is sufficient to prevent back transfer to SP*, but it does so with a minimum (exothermic) energy loss. In fact, $\Delta\Delta E$ is just large enough that fluctuations in $\Delta E(t)$ do not reach values of $\Delta E(t) = 0$ (i.e., values suitable for back transfer to SP*). The calculated value of $\Delta\Delta E$ is relatively insensitive to the charge distributions used for neutral and ionic chromophores. Transfer to the ground state of the special pair appears to be prevented by the large energy gap, though it is not considered here.

The description of electron transfer controlled by fluctuations of $\Delta E(t)$ is closely related to the Marcus theory (36, 39). In fact, the mean and rms deviation and the time scale of the fluctuations (relaxation time of autocorrelation function) of $\Delta E(t)$ can be identified with parameters of that theory (36). With the assumption of displaced harmonic effective potential energy surfaces of the same form for the ionic and the neutral state, the Marcus theory reorganization energy (6) λ is equal to $\Delta\Delta E/2$. The results in Fig. 3 correspond to a value of $\lambda = 4.25$ kcal/mol. Our earlier calculations (23, 24) based on the 3-Å resolution structure yielded a value of $\lambda = 5.75$ kcal/mol, but otherwise displayed the same behavior (23, 24). The difference, 1.5 kcal/mol, between these two λ values provides an estimate for the errors in $\Delta\Delta E$ of our calculation. The present results are close to those of Creighton *et al.* (30) (5 ± 2 kcal/mol) for the corresponding reorganization energy in *Rb. sphaeroides*.

To determine the origin of the stabilization of the product state, we examined the electrostatic energy contributions of the different protein components to $\Delta\Delta E(t)$. In Table 1 these contributions are shown for a time point at which $|\Delta\Delta E(t)|$ is small (see Fig. 3) and for the average $\Delta\Delta E(t)$. The contributions are widely distributed. They arise from atoms belonging to the backbone, to the side chains, to the special pair and to the pheophytin BPL, to the remaining prosthetic groups, and to water molecules inside the protein. The contributions of backbone, side chain, SP, and BPL are of the same magnitude and have the major effect on $\Delta\Delta E$. Water molecules and other chromophores make smaller contributions. Table 2 lists the residues that contribute more than 0.3 kcal/mol to $\Delta\Delta E(t)$. A total of 21 residues make such contributions; most groups are relatively close to the special pair or to BPL. Contributions from the groups SP and BPL are included in the table since we have divided the chromophores into central portions (the charge density of which is affected by the electron transfer) and peripheral portions (the latter add the energies listed).

Table 1. Electrostatic energy contributions of different atomic groups of the RC to minimum and average values of $\Delta\Delta E$

Group of protein atoms	Contribution, kcal/mol	
	$\Delta\Delta E_{min}$	$\Delta\Delta E_{ave}$
Backbone	−2.6	−4.3
Side chain	1.0	−2.1
SP and BPL	−1.8	−2.9
All others		
Chromophores	−0.5	0.1
Water	−0.8	0.3
Total	−4.7	−8.9

The calculations were based (*i*) on coordinate sets before and after electron transfer, which yield a minimum $|\Delta\Delta E|$ value ($\Delta\Delta E_{min}$), and (*ii*) on time-averaged structures of dynamics simulations before and after electron transfer ($\Delta\Delta E_{ave}$).

To test whether fluctuations and solvation by the protein matrix contribute to the distinctive behavior of the two nearly identical branches of photosynthetic RCs (7), we performed a simulation in which an electron was transferred from the special pair to the pheophytin of the nonfunctional branch (BPM). The structural changes and response of the protein matrix were found to be essentially the same as for the transfer to BPL (26); i.e., the solvation process does not seem to play a role in discriminating electron transfer along the functional and nonfunctional branches.

Since the photosynthetic RC can carry out the photoinduced charge separation at low temperatures (16), it is of interest to investigate if the stabilization of the product state persists when the temperature is decreased. Surprisingly, we found that the stabilization of the separated charge pair also manifests itself in a RC quenched to 10 K. The response of the quenched protein complex reflected by $\Delta E(t)$ is shown in Fig. 4. Although the fluctuations of $\Delta E(t)$ are significantly reduced in amplitude, as would be expected, the solvation behavior is the same as the one shown in Fig. 3 for the 300 K RC. Apparently, the forces induced by the charge separation are sufficient to induce the required rearrangements without thermal activation. The contributions to $\Delta\Delta E$ at low temperature resemble the results shown in Table 1.

Summary

The results presented here demonstrate that the motions of most of the photosynthetic RC complex are coupled to the electron transfer processes by Coulomb interactions. The

Table 2. Electrostatic energy contributions ($\Delta\Delta E_{group}$) of protein residues and water molecules

Name	Type	$\Delta\Delta E_{group}$, kcal/mol	Name	Type	$\Delta\Delta E_{group}$, kcal/mol
M183	Trp	−0.305	L153	His	0.324
M184	Leu	−0.97	L157	Val	−0.349
M188	Ser	1.18	L162	Tyr	0.616
M203	Ser	−0.548	L167	Trp	0.77
M209	Gly	0.343	L168	His	0.519
M211	Gly	0.337	L173	His	−1.01
L104	Glu	0.614	L238	Ser	−0.515
L118	Pro	−0.362	L244	Gly	−0.388
L120	Ala	−1.77	L248	Thr	−0.753
L121	Phe	−0.376	W011	H_2O	0.364
L124	Pro	0.473			

The first letter of the name of a residue specifies the protein subunit to which that residue belongs (to the L or M subunit or to the set of water molecules inside the RC).

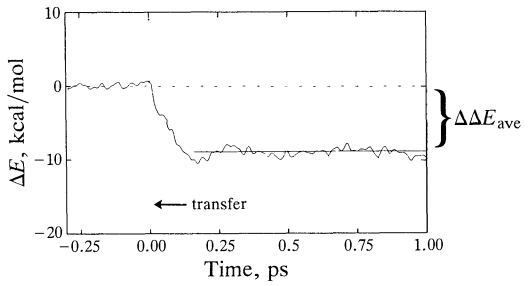

FIG. 4. Energy difference ΔE before and after electron transfer from the special pair to BPL calculated from a dynamics simulation of the RC quenched to 10 K. $\Delta\Delta E_{min}$, minimum $\Delta\Delta E$ value; $\Delta\Delta E_{ave}$, average $\Delta\Delta E$ value.

protein responds to electron transfer by an extremely fast (200 fs) dielectric relaxation, a response similar to solvation in polar liquids (40), except that the magnitudes of solvation energies are relatively small, presumably due to the weakly polar nature of the protein and the distributed charge in the chromophores. Thus, the thermal motion of the protein should play an important role in the control of electron transfer rates. Quantum mechanical calculations of coupled two-state systems with an energy difference $\Delta E(t)$ equal to that obtained from MD simulations of the photosynthetic RC support the important role of $\Delta E(t)$ in the electron transfer (36); the role of the much smaller fluctuations found at low temperature, most likely superseded by quantum effects, has yet to be determined.

The results also demonstrate the relatively delocalized nature of the dielectric fluctuations as well as the dielectric response of the photosynthetic RC. The protein backbone contributes to the stabilization along with many side chains. Thus, one cannot identify a single residue or a very small number of residues that dominate the solvation process, and there are not any large displacements that would be easily visible in structural studies. The result obviously has implications for the use of site-specific mutagenesis as a tool for probing the photosynthetic RC (41).

The rapid dielectric response to electron transfer is due to a shift of the potential minima of the charged atoms, which is so small that they can follow this shift almost adiabatically and do not need to overcome energy barriers to achieve the new equilibrium position; this is the reason that the solvation process at 10 K is very similar to solvation at room temperature. Quantum corrections that might be involved are not included in these classical simulations.

This work was supported by the Deutsche Forschungsgemeinschaft, F.R.G., and was carried out in part at the Center for Parallel Computation in Molecular Dynamics at the University of Illinois (funded by the National Institutes of Health). The work was supported also by grants from the National Science Foundation and the National Institutes of Health (M.K.). Computer time was granted by the National Center for Supercomputing Applications (supported by the National Science Foundation).

1. Wraight, C. A. & Clayton, R. K. (1974) *Biochim. Biophys. Acta* **333,** 246–260.
2. Kreider, J. F. & Kreith, F., eds. (1981) *Solar Energy Handbook* (McGraw–Hill, New York).
3. Marcus, R. (1956) *J. Chem. Phys.* **24,** 966–978.
4. Marcus, R. (1956) *J. Chem. Phys.* **24,** 979–989.
5. Marcus, R. A. & Sutin, N. (1985) *Biochim. Biophys. Acta* **811,** 265–322.
6. DeVault, D. (1984) *Quantum-Mechanical Tunneling in Biological Systems* (Cambridge Univ. Press, Cambridge, U.K.).
7. Deisenhofer, J., Epp, O., Miki, K., Huber, R. & Michel, H. (1984) *J. Mol. Biol.* **180,** 385–398.
8. Deisenhofer, J., Epp, O., Miki, K., Huber, R. & Michel, H. (1985) *Nature (London)* **318,** 618–624.
9. Deisenhofer, J. & Michel, H. (1989) *Science* **245,** 1463–1473.
10. Budil, D. E., Gast, P., Chang, C. H., Schiffer, M. & Norris, J. R. (1987) *Annu. Rev. Phys. Chem.* **38,** 561–583.
11. Allen, J. P., Feher, G., Yeates, T. O., Komiya, H. & Rees, D. C. (1987) *Proc. Natl. Acad. Sci. USA* **84,** 6162–6166.
12. Allen, J. P., Feher, G., Yeates, T. O., Komiya, H. & Rees, D. C. (1987) *Proc. Natl. Acad. Sci. USA* **84,** 5730–5734.
13. Parson, W. W. (1987) in *New Comprehensive Biochemistry: Photosynthesis*, ed. Amesz, J., pp. 43–61.
14. Kirmaier, C. & Holten, D. (1987) *Photosynthesis Res.* **13,** 225–260.
15. Breton, J., Martin, J.-L., Migus, A., Antonetti, A. & Orszag, A. (1986) *Proc. Natl. Acad. Sci. USA* **83,** 5121–5125.
16. Fleming, G. R., Martin, J. L. & Breton, J. (1988) *Nature (London)* **333,** 190–192.
17. Holzapfel, W., Finkele, U., Kaiser, W., Oesterhelt, D., Scheer, H., Stilz, H. U. & Zinth, W. (1989) *Chem. Phys. Lett.* **160,** 1–7.
18. Jortner, J. & Bixon, M. (1987) in *Protein Structure–Molecular and Electronic Reactivity*, eds. Austin, R., (Springer, New York).
19. Warshel, A. (1980) *Proc. Natl. Acad. Sci. USA* **77,** 3105–3109.
20. Kleinfeld, D., Okamura, M. Y. & Feher, G. (1984) *Biochemistry* **23,** 5780–5786.
21. Woodbury, N. W. T. & Parson, W. W. (1984) *Biochim. Biophys. Acta* **767,** 345–361.
22. Treutlein, H., Schulten, K., Deisenhofer, J., Michel, H., Brünger, A. & Karplus, M. (1988) in *The Photosynthetic Bacterial Reaction Center: Structure and Dynamics*, eds. Breton, J. & Vermeglio, A. (Plenum, London), pp. 139–150.
23. Treutlein, H., Schulten, K., Niedermeier, C., Deisenhofer, J., Michel, H. & DeVault, D. (1988) in *The Photosynthetic Bacterial Reaction Center: Structure and Dynamics*, eds. Breton, J. & Vermeglio, A. (Plenum, London), pp. 369–377.
24. Treutlein, H., Niedermeier, C., Schulten, K., Deisenhofer, J., Michel, H., Brünger, A. & Karplus, M. (1988) in *Transport Through Membranes: Carriers, Channels and Pumps*, eds. Pullman, A., Jortner, J. & Pullman, B. (Reidel, Dordrecht, The Netherlands), pp. 513–525.
25. Michel, H., Epp, O. & Deisenhofer, J. (1986) *EMBO J.* **5,** 2445–2451.
26. Treutlein, H. (1988) Ph.D. thesis (Technische Universität München, München).
27. Dewar, M. J. S. & Thiel, W. (1977) *J. Am. Chem. Soc.* **99,** 4899–4907.
28. Dewar, M. J. S. & Stewart, J. J. P. (1986) *Quantum Chem. Program Exchange Bull.* **6,** 24–32.
29. Warshel, A., Creighton, S. & Parson, W. W. (1988) *J. Phys. Chem.* **92,** 2696–2701.
30. Creighton, S., Hwang, J.-K., Warshel, A., Parson, W. W. & Norris, J. (1988) *Biochemistry* **27,** 774–781.
31. Warshel, A., Chu, Z. T. & Parson, W. W. (1989) *Science* **246,** 112–116.
32. Plato, M., Lendzian, F., Lubitz, W., Tränkle, E. & Möbius, K. (1988) in *The Photosynthetic Bacterial Reaction Center: Structure and Dynamics*, eds. Breton, A. & Vermeglio, A. (Plenum, London), p. 379.
33. Brooks, B. R., Bruccoleri, R. E., Olafson, B. D., States, D. J., Swaminathan, S. & Karplus, M. (1983) *J. Comp. Chem.* **4,** 187–217.
34. Brooks, C. B. & Karplus, M. (1989) *J. Mol. Biol.* **208,** 159–181.
35. Warshel, A. & Karplus, M. (1975) *Chem. Phys. Lett.* **32,** 11–17.
36. Schulten, K. & Tesch, M. (1991) *J. Chem. Phys.*, in press.
37. Plato, M., Möbius, K., Michel-Beyerle, M. E., Bixon, M. & Jortner, J. (1988) *J. Am. Chem. Soc.* **110,** 7279–7285.
38. Plato, M. & Winscom, C. J. (1988) in *The Photosynthetic Bacterial Reaction Center: Structure and Dynamics*, eds. Breton, J. & Vermeglio, A. (Plenum, London), p. 421.
39. Nonella, M. & Schulten, K. (1991) *J. Phys. Chem.*, in press.
40. Maroncelli, M., MacInnis, J. & Fleming, G. R. (1989) *Science* **243,** 1674–1681.
41. Bylina, E. J. & Youvan, D. C. (1988) *Proc. Natl. Acad. Sci. USA* **85,** 7226–7230.